A FRAMEWORK FOR GLOBAL VERIFICATION OF SPACE-BORNE RADAR ESTIMATES OF PRECIPITATION BASED ON RAIN TYPE CLASSIFICATION

Eyal Amitai[1,2,*], Xavier Llort[3], Liang Liao[1,4] and Robert Meneghini[1]

[1]NASA Goddard Space Flight Center, Greenbelt, Maryland, USA
[2]School of Computational Sciences, George Mason University, Fairfax, Virginia, USA
[3]GRAHI/Universitat Politecnica de Catalunya, Barcelona, Spain
[4]Caelum Research Corp., Rockville, Maryland, USA

1. INTRODUCTION

The distribution of *rain rates* (*R*) is of great interest in many fields. For example, hydrological applications such as flood forecasting depend on an accurate representation of the excess rainfall--driven by *R*--that does not infiltrate the soil. Better estimation of the spatial probability distribution function (pdf) of *R* is also crucial for better evaluation of rainfall products from space-based radars. The evaluation of instantaneous rainfall products and rain rate estimates from space is quite a challenge. Scatter plots of direct comparisons of rain rates with ground-based radar estimates (pixel by pixel) are extremely noisy because of sample volume discrepancies, timing and navigation mismatches, and uncertainties in the observed-radar reflectivity rain-rate Z_e-R relations. Furthermore, comparisons of rainfall over daily, weekly or even monthly time scales suffer from the temporal sampling errors of the satellite where the revisit time is on the order of hours or days (e.g., the Tropical Rainfall Measuring Mission [TRMM] satellite, the future Global Precipitation Measurement [GPM] mission satellite). Consequently, an alternative approach (Amitai et al. 2003) of comparing space-based radar pdfs with pdfs derived from co-located ground-based radar observations is attractive for evaluating satellite-based precipitation products, such as those from TRMM precipitation radar (PR).

A framework for physical validation of spaceborne radar estimates of rain rate has been developed. The framework demonstrates how a hydrologic approach that uses statistical properties of the precipitation to estimate the uncertainties can be combined with a meteorological approach that uses physical properties of the rainfall. It is based on comparing pdfs of *R* from ground-based and space-based radar observations. The framework includes the use of pdf comparisons before and after rain type classification. The classification will allow for better evaluation of the satellite algorithms under different conditions, and potentially will allow for "extrapolation" of the uncertainties to regions not covered by validation data sets but characterized by the same rain type. The framework also focuses on determining and reducing the uncertainties in the ground validation pdfs. This letter presents the results from initial comparisons of pdfs of rain rate from the TRMM PR and co-located data from the TRMM ground validation (GV) radar, obtained over central Florida during five years of observations. It provides a brief review of how well the TRMM satellite validation estimates compare to TRMM PR retrieved estimates.

2. COMPARISONS OF PDFS OF RAIN RATE FROM THE TRMM PR AND CO-LOCATED TRMM GV RADAR DATA

The pdfs shown here represent the distribution of rain volume by rain rate, i.e. they are constructed according to the relative contribution of each rain intensity to the total rain volume. Such pdfs are less sensitive to the instrument rain detection limits than the pdfs of occurrence, and have direct hydrological significance. The rain rates used to derive the pdfs are based on co-located TRMM PR and TRMM GV radar observations taken from a range interval of 15 to 100 km from the Melbourne, Florida National Weather Service Radar (WSR-88D). The rain rate estimates are taken from the NASA TRMM standard products (version 5) and pixel-matched in both time and space after averaging to the highest common horizontal resolution of 4x4 km^2.

Figure 1 presents a comparison of the pdfs based on all TRMM overpasses found during 5 years of mission over central Florida (105 overpasses during rain). Overall, PR underestimates the rain by 4% compared to the GV estimates. Calculation of rain amounts in situations in which one instrument detected rain and the other did not, reveals that 7.5% of the rain amount measured by the GV radar occurred in regions where the PR registered no rain. In these pixels the GV averaged R was found to be 1.8 mm/h as compared to the value 6.1 mm/h, based on all GV rainy pixels (*R*>0). Is it rain that cannot be detected by the PR due to its low sensitivity? We believe that this is in fact the case, although some of the discrepancy appears to be caused by registration errors. It was also found that 3% of the PR rain was detected in pixels in which the GV radar registered no rain, and was also characterized by weak rain rates (<*R*>=1.6 mm/h as compared to <*R*>=5.5 mm/h based on all PR rainy pixels). As a first-order estimate, we assume that of the 7.5% of the events where GV detects rain and the PR does not, 3% is associated with mismatches due to wind sorting and navigation and timing errors, while the remaining 4.5% is the result of the lower detection threshold of the PR relative to the GV. Assuming the GV radar estimates are truth, the comparisons suggest that the PR underestimates the rain by 4%, but also does not detect 4.5% of the rain. On the other hand, when the PR detects rain, it compares well with the ground radar estimates.

---

* *Corresponding author address:* Eyal Amitai, NASA Goddard Space Flight Center, Code 912.1, Greenbelt, MD 20771, USA Eyal.Amitai@gsfc.nasa.gov
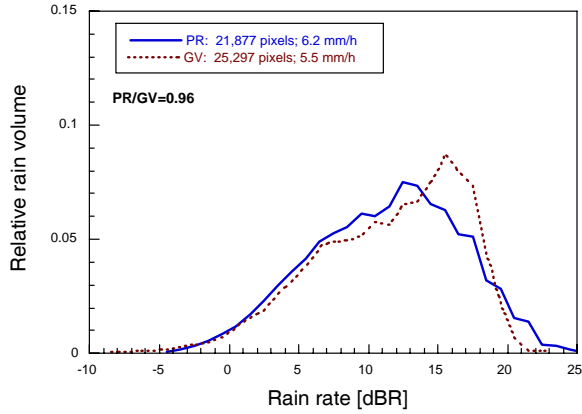
Fig. 1: Distribution of rain volume by R for the Melbourne, Florida, WSR-88D (GV) and TRMM PR datasets based on 105 overpasses during 1998-2002 and co-located GV data within 100 km of Melbourne. The GV R estimates are taken from TRMM standard product 2A-53 version 5 based on WPMM with 2x2 km^2 pixel resolution, averaged to 4x4 km^2. The number of rainy pixels, their averaged rain rate, and the PR/GV rain volume bias are indicated in the legend. Note, dBR=10 log(R/ 1 mm h^{-1}) | [R]=[mm h^{-1}].

Explanation for the shift in the GV pdf curve toward high rain rates at low and medium rain intensities and vice versa for higher rain intensities, as seen in figure 1, requires further analysis. An analysis based on rain type classification will be described in the following section.

The NASA TRMM satellite validation program recently switched from producing ground-based radar rainfall products based on the gauge adjusted power law $Z_e=AR^b$ relations with a fixed b of 1.4 to those based on the window probability matching method (WPMM, Rosenfeld et al.1994). The GV R estimates based both on the WPMM and on the power law are shown in figure 2. Which curve better represents the truth? Based on sensitivity analysis of the GV pdfs, Amitai et al. (2004) have demonstrated that uncertainties in the derived ground-based radar pdfs are likely to be smaller when using a gauge-based R distribution (V5) rather than employing an adjusted power law relation (V4). However, the similarity between the two GV curves, along with the sensitivity tests for estimating the uncertainties in the derived GV pdfs (Amitai et al. 2004), increase our confidence that the major differences between the PR and the GV pdfs which remain after switching to version 5 are due to satellite algorithm error. In this example, the overestimation is probably due to over-correction of attenuation by the TRMM PR algorithms. Further analysis has shown that only one or two overpasses dominated the high end of the PR rain distribution. Moreover, the pdfs based on the 19 rainy overpasses found in the following year (1999) reveal the opposite trend where the PR distribution is shifted toward lower R relative to the GV distribution (i.e., PR overestimates probabilities of low R, and underestimates probabilities of high R), as seen in figure 3. To attempt to better understand this discrepancy we consider below classifying the data by rain type.
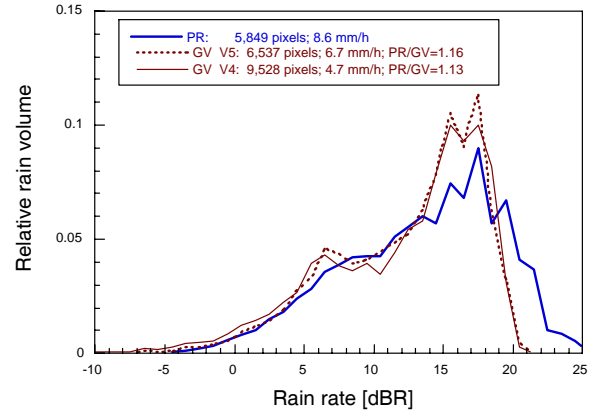

Fig. 2: Distribution of rain volume by R for the Melbourne, Florida, WSR-88D (GV) and TRMM PR datasets based on 24 overpasses during 1998 and co-located GV data within 100 km of Melbourne. The GV R estimates are taken from TRMM standard product 2A-53 version 5 (V5) and version 5 (V5) based on WPMM and version 4 (V4) based on a power law with 2x2 km^2 pixel resolution, averaged to 4x4 km^2.

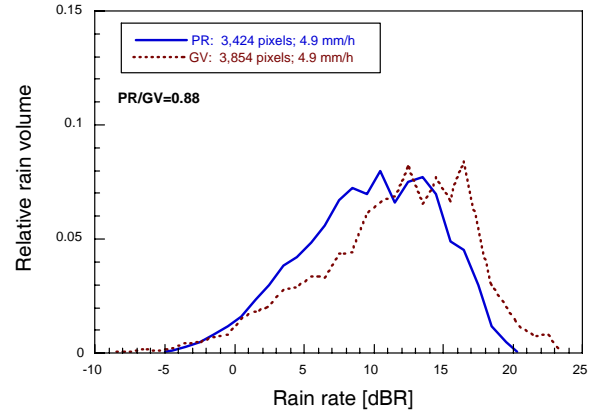

Fig. 3: Same as figure 1, but based on 19 overpasses during 1999.

3. COMPARISONS OF PDFS AFTER RAIN TYPE CLASSIFICATION

In this study, the Amitai (1999) classification scheme is used. This classification scheme--based on analyzing simulated TRMM PR 3-D reflectivity field structure using ground based radar data--defines fourteen rain types, each characterized by a unique pdf of near surface reflectivities and a mean R (see Figure 2 and Table 2 in Amitai 1999). Based on physical principles it uses the following parameters for classification: Echo top height at 20 and 32 dBZ, horizontal reflectivity gradients above the freezing level, and the strength of the bright band signature. Parameters such as these are basically determined by the degree of morphological organization of the rain system and their static instability. The reflectivity value of 20 dBZ was chosen as an approximation to the minimum detectable
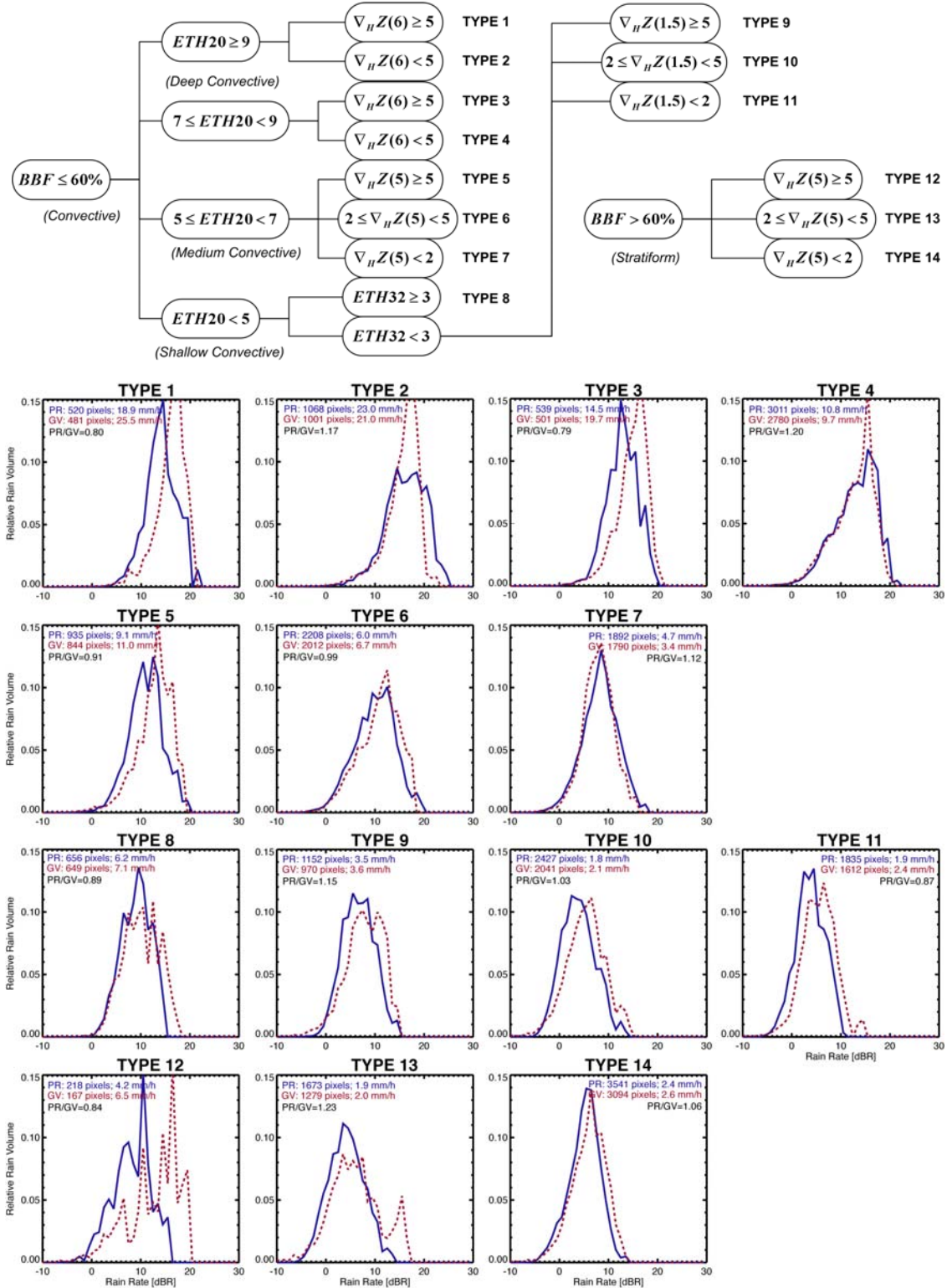
Fig. 4: Top: The classification chart used to classify the rain (after Amitai 1999). Horizontal reflectivity gradients $\nabla_H Z(n)$, in dB/4km, are calculated at n km above surface. Echo Top Height of 20 and 32 dBZ (ETH20, ETH32) in units of km above the surface. Bright Band Fraction (BBF) of 0.6 is used for convective/stratiform separation. Below chart: The pdfs using all 105 overpasses over central Florida, as in figure 1, but for each of the fourteen types separately. The number of rainy pixels, their averaged rain rate, and the PR/GV rain volume bias are indicated in the legends (PR- solid curve, GV- broken curve).

signal of PR. Reflectivities less than 32 dBZ were assumed to be unaffected by attenuation.

The pdfs for each of the Amitai (1999) rain types, using data from all 105 overpasses are presented in Figure 4. The classification scheme is applied to the PR data set, while the GV data set is classified based on PR-GV matched-pixels. For most rain types, the PR pdfs are shifted toward low R relative to the GV pdfs (i.e., PR overestimates probabilities of low R, and underestimates probabilities of high R). PR overestimation at high R (i.e., PR pdf shifted toward high R relative to the GV pdf) is found only in three of the rain types (types # 2, 4 and 7). In these rain types the echo top heights usually exceeded 9 km, always exceeded 5-km, and a bright-band signature did not exist (i.e., very convective cells). However, they were also characterized by weak horizontal reflectivity gradients. Weak horizontal gradients suggest that partial beam filling is not an issue. On the other hand, in heavy convection, a significant contribution to the total attenuation can arise from mixed phase particles; underestimating the fraction of the attenuation caused by the mixed phase region and overestimating the attenuation caused by cloud water can yield overestimates of near-surface rain. This is also supported by a higher $<R>$ compared to that of the GV for these classes only. These three types combined, contributed about half of the total rain amount (49% of the total PR rain and 40% of the total GV rain). In these cases the PR exceeded the GV by 18%. For all other rain types combined, the PR underestimated the rain by 18%. The total GV and PR rain estimates do not balance out (fig. 1) since each is not exactly contributing to 50% of the total rain. The $<R>$ for each rain type, and the trend in the $<R>$ observed from type-to-type in the GV data set is in accordance with the results from the simulation performed by Amitai (1999). For example, type #2 had a lower $<R>$ than type #1, as expected. This is not the case for the PR. Does this suggest that GV is more representative of the truth? Both the simulations (Amitai 1999) and the sensitivity tests (Amitai et al. 2004) increase our confidence in the GV estimates beyond those of the PR for the example given here, however, in general, we have to look for possible errors and error sources in both GV and PR estimates.

4. SUMMARY

A comparison of rain rate estimates from the TRMM PR and TRMM GV radar based on 53 months of observations over central Florida is provided. Overall, the PR underestimates the rain by 4%, but also does not detect 4.5% of the rain as compared to the GV radar. Results from initial comparison of pdfs of rain rate from TRMM PR and TRMM GV estimates demonstrate how well the TRMM satellite validation pdfs compare to TRMM PR retrieved estimates. This comparison effort is part of a developing framework for physical validation of spaceborne radar estimates of rain rate. The framework includes the use of pdf comparisons before and after rain type classification. The classification allows for better evaluation of the satellite algorithms under different conditions, and potentially will allow for "extrapolation" of the uncertainties to regions not covered by validation data sets but characterized by the same rain type. The framework also focuses on determining and reducing the uncertainties in the GV pdfs. While uncertainties in the determination of the ground-based radar pdfs are reduced upon adjustment with those from gauge data (Amitai et al. 2004)--a major motivation for NASA TRMM validation program's product generation based on WPMM Z-R relations--utilizing super dense gauge network for accuracy verification of the derived pdfs will further reduce the uncertainties.

6. REFERENCES

Amitai E, Nystuen JA, Liao L, Meneghini R, Morin E. 2004: Uniting space, ground and underwater measurements for improved estimates of rain rate. *IEEE Geoscience and Remote Sensing Letters,* **1**, 35-38. DOI: 10.1109/LGRS.2004.824767.

Amitai E, Liao L, Wolff DB, Marks DA, Silberstein DS. 2003. Challenges and proposed solutions for validation of rain rate estimates from space. *IEEE International Geosciences and Remote Sensing Symposium 2003,* **3**, 1966-1968 on CD-ROM ISBN: 0-7803-7930-6, Toulouse, France.

Amitai E. 1999. Relationships between radar properties at high elevations and surface rain rate: potential use for spaceborne rainfall measurements. *J. Appl. Meteor.,* **38**, 321-333.

Rosenfeld D, Wolff DB, Amitai E. 1994: The window probability matching method for rainfall measurements with radar. *J. Appl. Meteor.,* **33**, 682-693.